Development and Tests of Silicon Strip Modules for the ATLAS Upgrade

DESY Summer Student Programme, 2014

XIANG Xiaoyu

Tsinghua University, China

Supervisor
Ingo Bloch

5th of September 2014

Abstract

The ATLAS inner detector upgrade process is aimed to meet the requirements posed by exposure to high irradiation and other condition in the high level of luminosity Large Hardron Collider (HL-LHC). A new strip-based semi-conductor detectors will be required.

This report covers an experiment where a Silicon strip-module is tested with an improved testing system in the environment created by a climate chamber. Even though the general observation shows the exceptional decrease of the module noise level with reduced temperature. Some irregularities in the noise response were observed. These indicate an additional so far not well controlled source of noise in the modified setup.

清華大學
Tsinghua University

Contents

1 Introduction

1.1 ATLAS Detector

The ATLAS detector is a general purpose experiment designed to identify and precisely measure the energies and momenta of the particles produced in the collisions, which happen in the Large Hardron Collider (LHC)[1]. The ATLAS detector contains several different layers with cylindrical and forward-backward symmetry with respect to the interaction point. The Inner Detector (ID) is used to measure the trajectories of charged particles emerging from the LHC collisions.

It is expected that the LHC physics program will be upgraded with increased peak luminosity up to $10^{35} cm^{-2} s^{-1}$ by 2023. The integrated luminosity per experiment after the HL-LHC upgrade will be approximately $3000 fb^{-1}$[3]. The goal of the upgrade of the LHC and the ATLAS detector is to reduce the statistical errors and provide access to unexplored region of phase space.

The higher luminosity of the HL-LHC will cause higher occupancies of the detectors and higher irradiation. Therefore, it is necessary to upgrade the detector to get higher granularity of detection, to improve the radiation hardness, and to introduce new powering schemes to account for the number of increasing electronic channels due to the higher granularity of the detector.

In the evolution of ATLAS Tracker, there are two main challenges that are needed to be overcome for the detectors to cope with the HL-LHC: Pile-up events and their corresponding large impact on occupancies, and Radiation damage[11].

At present the major parts of the Inner Detector are Silicon pixel and strip detectors, and transition radiation trackers, which would be replaced by an all-Silicon tracker after the upgrade[12]. The reason to replace the entire ID is that the Transition Radiation Tracker at larger radii will suffer from a prohibitively large occupancy. Furthermore the Semiconductor Tracker and Pixel Detectors at smaller radius will get reduced performance by radiation damage of the sensors and the front-end electronics[11].

The current baseline layout of the Inner Detector is shown in Figure 1.

1.2 Silicon Strip Sensor

The Silicon sensors work to measure the tracks of ionized particles by the generation of electron-hole pairs in the depleted zone (shown in Figure 2).

The Silicon is chosen because of characteristics like small band gap, high specific density, and high carrier mobility. While the Silicon detectors currently used on ATLAS are p-in-n sensors, which means that the segmentation is an implant of p+ strips on the n- basis. The upgrade tracker will be made using n+ in p- sensor technology, which has become accessible in recent years and is more radiation tolerant.

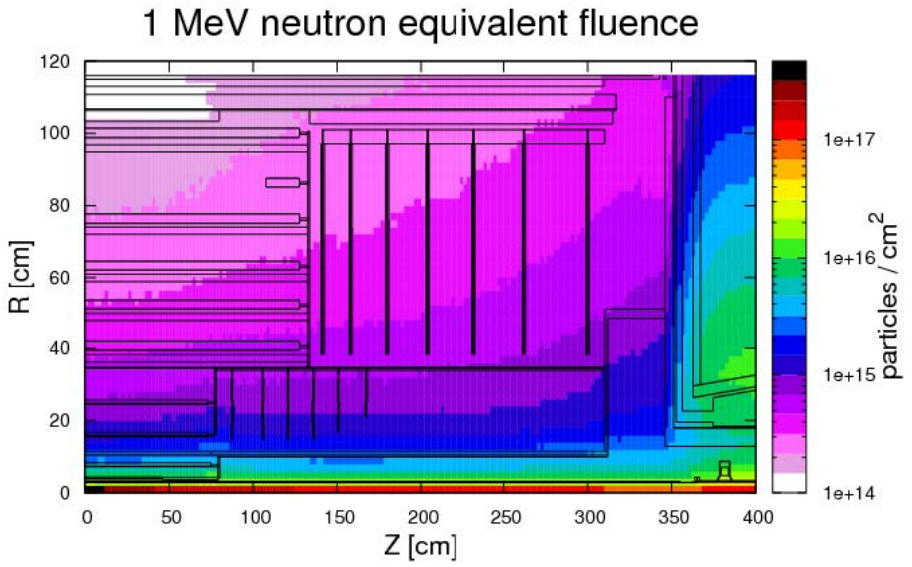

Figure 1: Detector layout with 1 MeV n_{eq} fluences for the ID region

By applying an external voltage in the reverse bias direction, a depletion zone can be created. The reverse bias gives rise of a small current, leakage current, which contributes to electronic noise and a consequent degradation in the signal-to-noise ratio of the output pulse.

1.3 Input Noise

The input noise of the detector includes the noise from the amplifier and capacitance of the fully depleted strip, and the thermal noise.

The depleted semiconductor could be regarded as a capacitor, where the resistance functions as not only a noise source but a filter as well[4]. The mean-square and RMS noise voltage in such RC circuit can be expressed by equation 1.

$$\bar{v_n^2} = \frac{k_B T}{C} \tag{1}$$

According to equation 1, the thermal noise can be decreased under lower temperature.

When applied with high bias-voltage, silicon the semiconductor might be fully depleted, which would minimize the capacitance of it and reduce the numerator of the equation 1. Accordingly, equivalent capacitance noise and thermal noise decrease meanwhile[9].

The noise is measured through a test called 3 Point Gain test that scans over different threshold voltages for every readout channel. By analyzing the relation between the injected charge and the response Vt50, the gain could be obtained. With the result of output noise (σ_s), the input noise(innse) is obtained[7]:

$$Innse = 6250 \times \frac{\sigma_s}{gain} \tag{2}$$

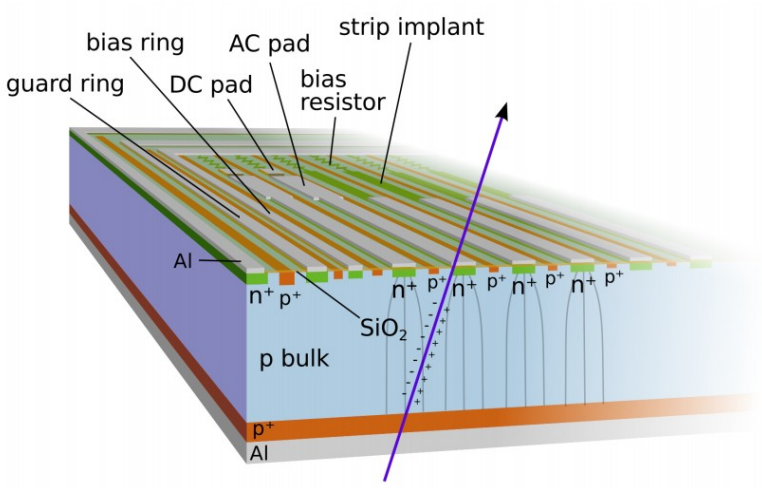

Figure 2: Cross-section of a Silicon strip detector and representation of signal formation[10]

1.4 Module Layout

Each module hosts a 97.54 × 97.54 mm^2 large Si microstrip sensor[2], which integrate four rows of 1280 strips of 23.82 mm in length. Twenty ABCN readout chips are placed on each of two hybrids that distributes I/O data and electric power to the ASICs and glued directly onto the Silicon sensor. The conceptual layout and photo of a module is shown in Figure 3.

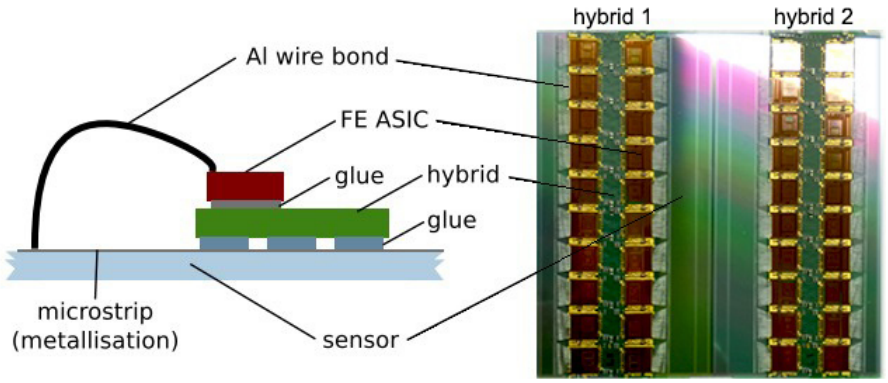

Figure 3: Conceptual layout of a single-sided module at the cross-section profile (left) and real photo of top view (right)

The Silicon sensor, ABCN chips and hybrids are produced by several different institutes and assembled at DESY. The mechanical connections of different components are provided by UV glue and Kapton layers, which are supposed to function well under the high-radiation in a wide temperature range. Wire-bonds between the Silicon sensor and the readout system ensure the electric connections. The construction of a module commonly consists of these steps:

1. Gluing of the readout ASICs onto hybrids;

2. Wire-bonding of ASICs to hybrids;
3. Electrical testing on hybrids;
4. Quality tests on sensors;
5. Gluing of hybrids onto sensors;
6. Wire-bonding of ASIC readout cells to single strips on the sensors;
7. Final electrical and mechanical testing of modules.

2 Module Testing

A module is tested by measuring the noise of the channels at different temperatures and voltages. All the actions are carried in a clean and dust-free test environment provided by laminar flow tent.

Figure 4: Climate chamber with a glass dummy module mounted onto a vacuum chuck

2.1 Testing Device Setup

The whole module is attached onto a vacuum chuck which provides the necessary connection of the bias-voltage to the sensor, and the mechanical support and vacuum holes for securely fixing and providing good thermal and electrical contact of the module as well as its PCB frame. The aluminum chuck also serves as a common grounding point for the low voltage(ASIC power) and the high voltage(bias-voltage for the Silicon sensor) circuit.

Besides, some peripheral equipment are applied: some silica-gel desiccant packs and a dried nitrogen tube are put near the chuck in the climate chamber to lower the humidity down, which contributes to control the dewpoint around the chuck inferior to the exact temperature and keep frosts or water drops from gathering on the module; to accelerate the air flow a fan is placed inside of the chamber. According to the results based on monitoring, the intervention of fan flattens the hybrid temperature graph at the turning points.

2.2 Fracture of the First Module

Each module hosts a $97.54 \times 97.54 mm^2$ large Silicon microstrip sensor. Figure 3 shows a conceptual layout of a single-sided module. The linear thermal expansion coefficient σ changes with the temperature and these layers made of different materials have a very high variation: The silicon is $2.56 \times 10^{-6} K^{-1}$[5] and the copper is $17 \times 10^{-6} K^{-1}$.

When the bias-voltage is applied and the ABCN chips are powered, the distributed resistance in the system would produce extra heat. The heat generated by the hybrid is unequally distributed. During the experiment the environmental temperature can be as low as -40 ℃, under that circumstance the thermal expansion as well as the unequally heat distribution would apply relatively large stress on the module. The euqation 3.

$$F = S \times E \Delta T \sigma \tag{3}$$

where S = cross-section area
E = Young's modulus
ΔT = temperature variation
σ = linear thermal expansion coefficient[8]

Assuming the temperature varies from 20 ℃ to -40 ℃, and the cross section area of the hybrid is $0.274mm \times 24mm$, the forces can be estimated with equation 3: $F_{Cu-Si} = 634.01N$, $F_{Cu-glass} = 126.8N$. In the actual experiment, the temperature drop results in a shattered Silicon sensor as shown in figure 5. Because the tests are carried in a light-tight chamber, the specific process of the fracture is not recorded. Based on former observations and crack condition, some hypothesis are made to explain the fracture:

1. The thermal stress residing in different materials surpass the reasonable range;
2. The heat's unequal distribution produces shear stresses between regions with temperature differences;
3. As a result a region of stress concentration is created in the sensor.

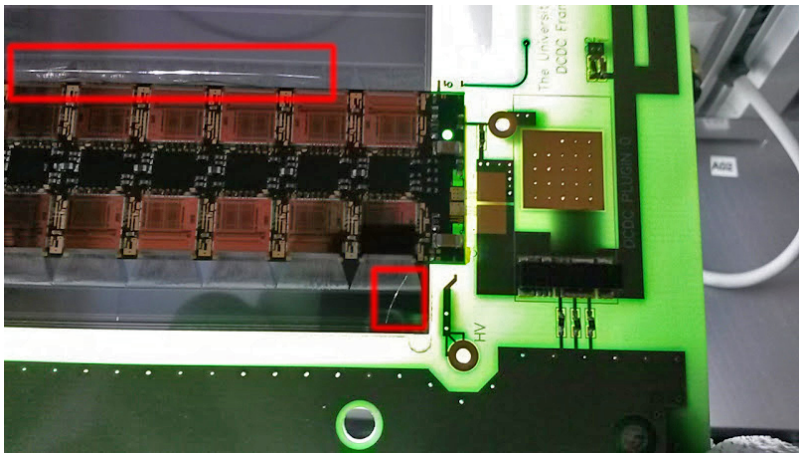

Figure 5: Shattered Silicon sensor with cracks on the top left and bottom right corner

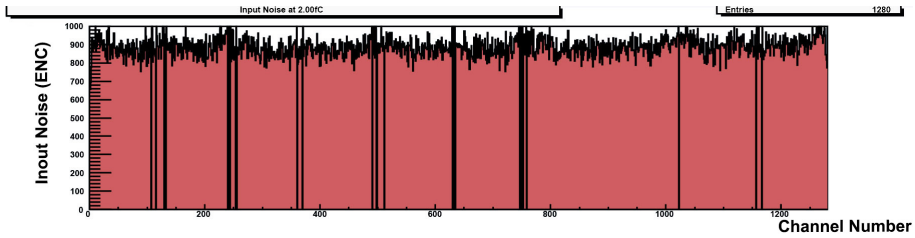

Figure 6: Noise spectrum of all channels in one row

2.3 Noise Measurement

The bias-voltage varies between 0V to -100V considering the safety of the module and the testing time. And the environmental temperature created by the climate chamber could be down to -20 ℃[1]. A ROOT[6] script is employed to get the current parameters (high voltage, temperature, current and humidity), set the bias-voltage and target temperature, and switch the devices on or off.

To start with the test, the so-called BCC (Buffer Control Chip) Startup should be carried out firstly to configure the BCC and chips of the modules. After that a series of 3 Point Gain tests are done under different set points. In the following experiments, the target temperatures are (15,5,-10,-15)℃[2] and the bias-voltages are (-10,-20,-30,-45,-50,-60,-80,-100)V. Before starting the measurements of each temperature, we wait for 30 minutes to ensure the temperature curve of chuck and hybrids fully stabilized. The data of two hybrids are saved independently and plotted with different colors in the following graph.

3 Result and Analysis

Among all the 2560 channels per hybrid, over 95 percent acted well (neither high-noise nor dead) during the experiment. All these noise originates from a lot of independent random events, so statistically they show a nearly Gaussian distribution (shown in Figure 7(a)). However, when examining the noise spectrum on all the channels (Figure 3), there is an obvious fluctuation where the wave crests (and dead channels) locate near the edge of each chip (multiples of 128). When cutting these malfunctioning channels, the average noise decreases in a small range (Figure 7(b)).

Eliminating the channels on the edge of the chips only moves the noise distribution as a whole, but not changes the relative position in the Voltage-Noise or Voltage-Current graphs. So the following graphs and analysis are based on the uncut results. Within the range of 15℃ to -15℃ of the environmental temperature, it shows a negative correlation in the overall trend of average input noise influenced by bias-voltage(absolute value) in Figure 8. Although accompanied with some fluctuations, the noise decreases while the bias-voltage is boosted. Besides, the first derivative (or the change rate) of noise also decreases with the voltage arise, which can result in approaching the full depletion voltage.

[1]The Silicon sensor of the last module cracked when the temperature went down to or rose up from -40 ℃. Considering this the temperature in the following tests should be far from that point

[2]When attempting to cool down to -20℃, we lost the current signal because the module bent badly and lost the contact with the touch spot.

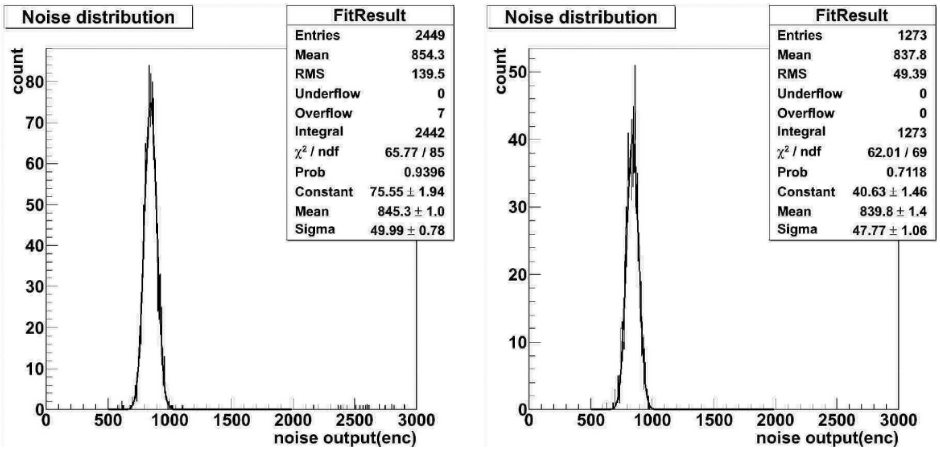

(a) Noise distribution of all active channels (b) Noise distribution without channels on the edge of each chip

Figure 7: Average noise varies with regard to bias-voltage and temperature

When the absolute bias-voltage higher than 80V, the change doesn't seem to have obvious effects on the average input noise.

To be noted, except for the Figure 8(a), all the other graphs in Figure 8 have some abnormal fluctuations, which could also be seen in the former tests. One of the possible explanation for this is the instability of experimental environment: the noise interference from surrounding electronic devices, the uncontrolled humidity below 10 ℃, and the possible poor contact because of the bending caused by different materials' contracts during cooling down.

Figure 9 shows the dependence of average input noise on both bias-voltage and temperature. In the range of experiments the influence of bias-voltage weights more than the temperature. Even so, the local influence of temperature doesn't so conform to each other, which is perhaps because of the data points are taken before the chuck/hybrid's temperature stabilize.

4 Conclusion

The former module cracked when cooling down to -40 ℃, and the later module lost the signal of current because of the upwarp of module at -20 ℃. Considering the temperature could range from -40 ℃ to 75 ℃ (heat up to dehumidify before cooling down), the thermal stress and deformation are needed to be calculated when dealing with bonded layered-frames.

The Silicon strip module rebuilt later has been proved to be proper functioning in the tests above. Preliminary results show comparatively high noise of the module, which may result in the overlap of wire-bonding and imperfect grounding. The overall trend of output noise generally meet our expectations, though some irregularities are observed. It

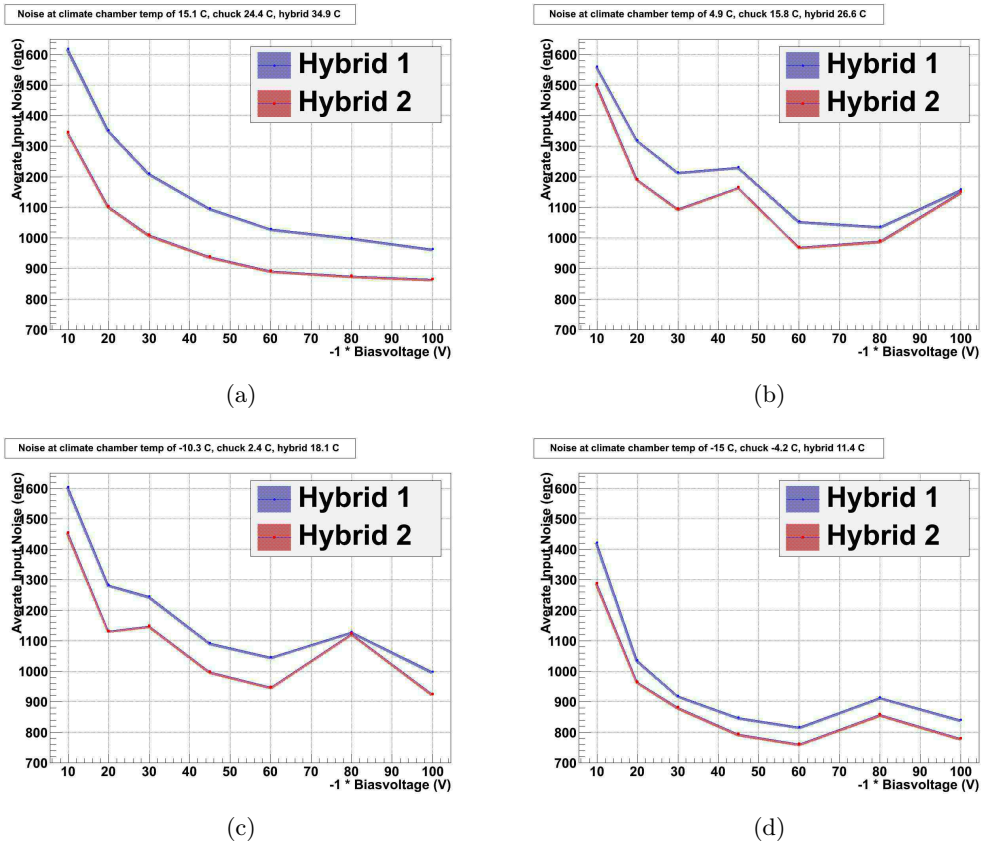

(a) (b) (c) (d)

Figure 8: Dependence of input noise on the bias-voltage at different temperatures

still needs more works to settle the uncontrolled noise soure and improve the supporting structure.

Acknowledgements

I wish to offer my sincerest gratitude to my supervisor, Dr. Ingo Bloch, who has supported me with his patience and knowledge. Mr. Dennis Sperlich and Dr. Kristin Lohwasser are thanked for the generous guidance and help. Thanks to many people who provided help and support during these months, not only in the research field but also in every aspect of life as a summer student in DESY.

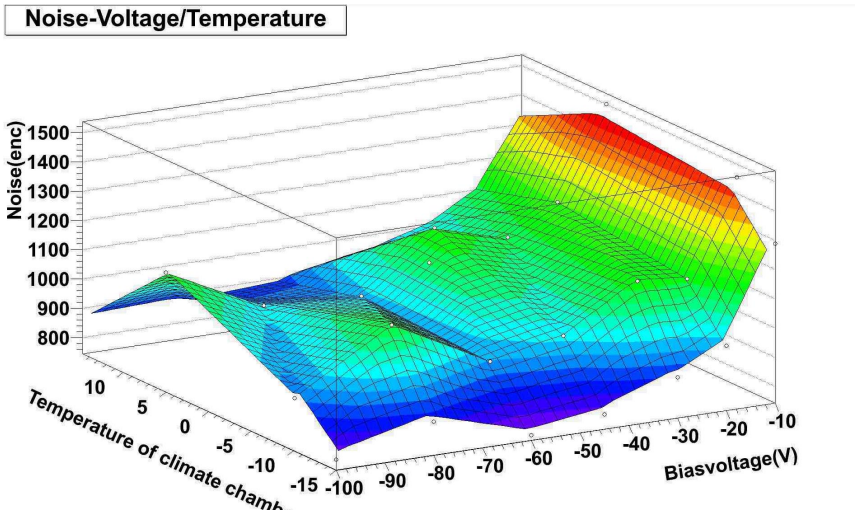

(a) Climate chamber

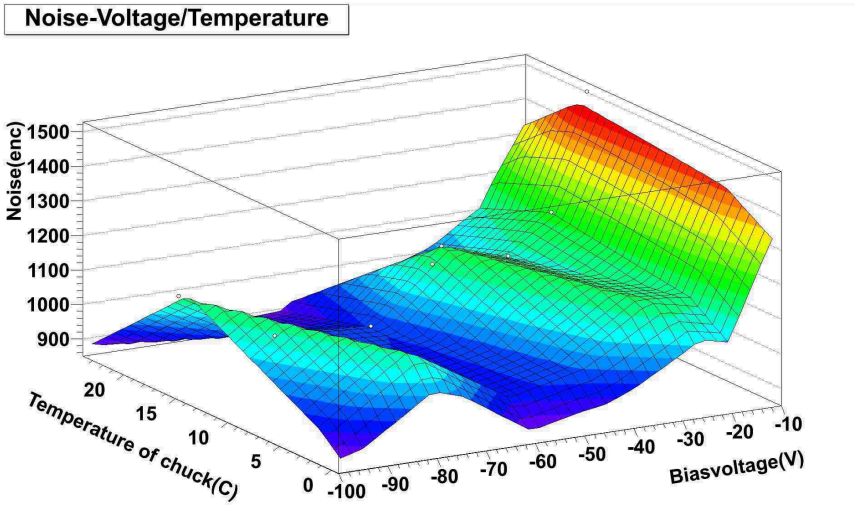

(b) Chuck

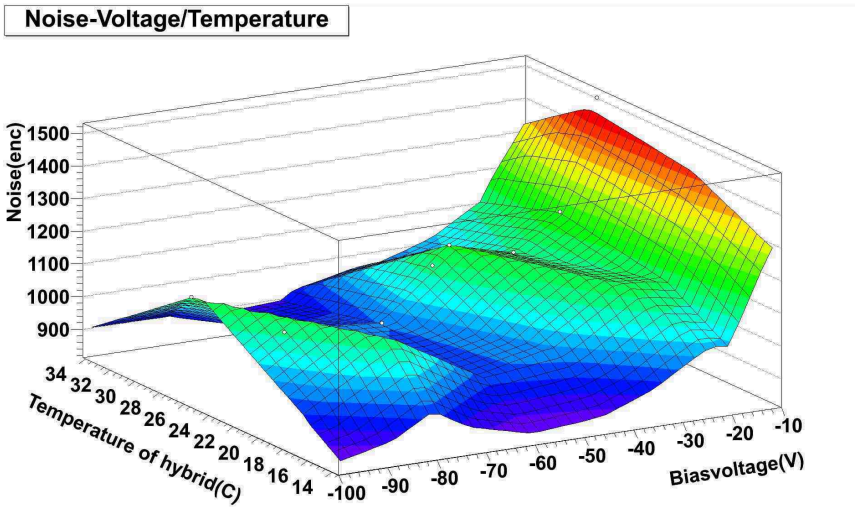

(c) Hybrid

Figure 9: Average noise varies with regard to bias-voltage and temperature (Original data shown as o dots)

References

[1] Georges Aad, E Abat, J Abdallah, AA Abdelalim, A Abdesselam, O Abdinov, BA Abi, M Abolins, H Abramowicz, E Acerbi, et al. The atlas experiment at the cern large hadron collider. *Journal of Instrumentation*, 3(08):S08003, 2008.

[2] PP Allport, AA Affolder, F Anghinolfi, R Bates, C Betancourt, C Buttar, JR Carter, G Casse, H Chen, A Chilingarov, et al. Progress with the single-sided module prototypes for the atlas tracker upgrade stave. *Nuclear Instruments and Methods in Physics Research Section A: Accelerators, Spectrometers, Detectors and Associated Equipment*, 636(1):S90–S96, 2011.

[3] Collaboration ATLAS. Letter of intent for the phase-ii upgrade of the atlas experiment. Technical report, 2012.

[4] John R Barry, Edward A Lee, and David G Messerschmitt. *Digital communication*. Springer, 2004.

[5] P Becker, P Scyfried, and H Siegert. The lattice parameter of highly pure silicon single crystals. *Zeitschrift für Physik B Condensed Matter*, 48(1):17–21, 1982.

[6] CERN. Root | a data analysis framework.

[7] Bilge Melahat Demirkoz. *Construction and performance of the ATLAS SCT barrels and cosmic tests*. PhD thesis, Oxford U., 2007.

[8] Richard B Hetnarski and M Reza Eslami. *Thermal Stresses–Advanced Theory and Applications: Advanced Theory and Applications*, volume 158. Springer, 2008.

[9] Glenn F Knoll. *Radiation detection and measurement*. John Wiley & Sons, 2010.

[10] John S Lilley. *Nuclear physics: principles and applications*. John Wiley & Sons, 2013.

[11] Tai-Hua Lin. Tests of silicon strip modules for the upgrade of the atlas detector at the lhc. Master's thesis, University Leipzig, the Deustchland, 2011.

[12] Hartmut F-W Sadrozinski. Tracking detectors for the lhc upgrade. *Nuclear Instruments and Methods in Physics Research Section A: Accelerators, Spectrometers, Detectors and Associated Equipment*, 552(1):1–6, 2005.